Published in final edited form as:
*Cancer Cell*. 2003 January ; 3(1): 75–88.

# Loss of pVHL is sufficient to cause HIF dysregulation in primary cells but does not promote tumor growth

**Fiona A. Mack**[1], **W. Kimryn Rathmell**[1], **Andrew M. Arsham**[1,2], **James Gnarra**[3], **Brian Keith**[1], and **M. Celeste Simon**[1,2,4]

[1]Abramson Family Cancer Research Institute, University of Pennsylvania School of Medicine, Philadelphia, PA 19104

[2]Howard Hughes Medical Institute, University of Pennsylvania School of Medicine, Philadelphia, PA 19104

[3]Department of Biochemistry and Molecular Biology, Louisiana State University Medical Center, New Orleans, LA 70112

## Summary

Inactivation of the von Hippel-Lindau (*VHL*) gene is associated with the development of highly vascularized tumors. pVHL targets the α-subunits of Hypoxia Inducible Factor (HIF) for ubiquitin-mediated degradation in an oxygen-dependent manner. Although pVHL-deficient tumor cell lines demonstrate constitutive stabilization and activation of HIF, it has yet to be shown that loss of murine *Vhl* alone is sufficient to dysregulate HIF. We utilized a genetic approach to demonstrate that loss of *Vhl* is sufficient not only to stabilize HIF-α subunits under normoxia, but also fully activate HIF-mediated responses. These studies have implications for the hierarchy of signaling events leading to HIF stabilization, nuclear translocation, and target gene expression. We further demonstrate that loss of murine *Vhl* does not promote teratocarcinoma growth, indicating that other genetic changes must occur to facilitate *Vhl*-mediated tumorigenesis.

## Introduction

von Hippel-Lindau disease is an autosomal dominant hereditary cancer syndrome. Patients heterozygous for one inactivating mutation within the von Hippel-Lindau (*VHL*) gene are predisposed to the development of pheochromocytomas and a variety of highly vascularized tumors, including renal clear cell carcinomas, retinal angiomas, and hemangioblastomas (Maher and Kaelin 1997). Within these tumors the second *VHL* allele has been rendered inactive by deletions, mutations, or hypermethylation. *VHL* is therefore a classic tumor suppressor conforming to the Knudson two hit hypothesis in which the second inactivating mutation occurs within somatic cells. A majority of sporadic renal clear cell carcinomas also exhibit biallelic loss of *VHL* function, further supporting *VHL*'s role as a tumor suppressor (Foster *et al.* 1994; Gnarra *et al.* 1994). Animal models demonstrate that deletion of murine *Vhl* function results in lethality, as $Vhl^{-/-}$ mice die *in utero* between E10.5-12 due to

[4]Correspondence: M. Celeste Simon, Howard Hughes Medical Institute, Abramson Family Cancer Research Institute, BRB II/III Rm. 456, 421 Curie Blvd., Philadelphia, PA 19104, TEL: 215-746-5562, FAX: 215-746-5532, celeste2@mail.med.upenn.edu.

placental vascular abnormalities (Gnarra *et al.* 1997). Hepatocyte-specific loss of *Vhl* in adult mice results in the formation of hemangiomas within the liver, a phenotype rarely observed in human *VHL* patients (Haase *et al.* 2001).

pVHL, the protein product of the *VHL* gene, interacts through its α-domain with elongins B/C and Cul2 to form the VBC complex, an E3 ubiquitin ligase. This multi-protein complex targets proteins for ubiquitin-mediated degradation, analogous to the *S.cerevisiae* SCF (Skpl/Cdc53/F-box) ubiquitination machinery (Pause *et al.* 1997; Lonergan *et al.* 1998; Lisztwan *et al.* 1999). Although pVHL has no sequence homology to any known proteins, it is functionally similar to the F-box protein of SCF by binding specific substrates through its β-domain (Ohh *et al.* 2000).

Major targets of the VBC complex include the regulatory α-subunits of the heterodimeric transcription factor Hypoxia Inducible Factor (HIF). HIF modulates both cellular and systemic responses to changes in oxygen ($O_2$) concentrations by stimulating the expression of genes involved in energy metabolism, angiogenesis, hematopoiesis and $O_2$ delivery. Proteasome inhibitor studies show that at high levels of $O_2$ (21%), the VBC complex binds HIF-α subunits (HIF-1α and HIF-2α), targeting them for ubiquitination and degradation via the 26S proteasome (Maxwell *et al.* 1999). Low $O_2$ (hypoxia) disrupts the association of pVHL with HIF-α subunits, which then dimerize with constitutively expressed ARNT/HIF-β to form transcriptionally active HIF. Mutations within the β-domain of pVHL disrupt its interaction with HIF-α subunits leading to constitutive HIF-α stabilization and HIF activity (Cockman *et al.* 2000; Ohh *et al.* 2000). Furthermore, *VHL*$^{-/-}$ renal clear cell carcinoma (RCC) cell lines fail to degrade HIF-α subunits under normoxic conditions. These cells display constitutive expression of HIF targets including genes encoding erythropoietin (EPO), vascular endothelial growth factor (VEGF), glucose transporter (GLUT-1) and phosphoglycerate kinase (PGK) (Iliopoulos *et al.* 1996; Maxwell *et al.* 1999; Krieg *et al.* 2000). In addition to its role as part of an E3 ubiquitin ligase, pVHL is required for proper fibronectin deposition, cytoskeletal reorganization and growth arrest upon serum withdrawal and contact inhibition, although the underlying mechanisms for these properties remain unclear. (Ohh *et al.* 1998; Pause *et al.* 1998; Hoffman *et al.* 2001; Kamada *et al.* 2001; Bindra *et al.* 2002). Defects within all of these pathways can be reversed by reintroduction of wild-type pVHL into *VHL*$^{-/-}$ RCC cells.

The interaction of pVHL with HIF-α is one of several $O_2$-dependent events thought to regulate HIF activity. First, pVHL binding to HIF-α subunits is dependent upon hydroxylation of key proline residues within the $O_2$-dependent degradation (ODD) domain of HIF-α (Ivan *et al.* 2001; Jaakkola *et al.* 2001). A recently defined family of HIF prolyl-hydroxylases (HTF-PHs) catalyzes this iron- and $O_2$-dependent reaction. All three elements of this pathway are conserved in *C. elegans, Drosophila* and mammals (Bruick and McKnight 2001; Epstein *et al.* 2001). Second, hypoxia is also believed to induce the nuclear accumulation of stabilized HIF-α subunits, protecting them from pVHL-mediated degradation (Kallio *et al.* 1999; Tanimoto *et al.* 2000). Third, hypoxia-mediated HIF transactivation of target genes requires interactions with coactivators p300 and CBP (Arany *et al.* 1996; Jiang *et al.* 1997; Pugh *et al.* 1997; Ebert and Bunn 1998; Carrero *et al.* 2000). Recent studies suggest that hydroxylation of a C-terminal activation domain (CAD)

asparagine residue by an iron- and $O_2$- dependent asparagyl hydroxylase disrupts HIF-α binding to coactivators p300 and CBP, thereby preventing transactivation during normoxia (Lando *et al.* 2002). Furthermore, hydroxylation within the CAD is thought to occur in a pVHL-independent manner (Sang *et al.* 2002). Therefore, under normal $O_2$ concentrations, hydroxylation of HIF-α on proline and asparagine residues regulates HIF's transcriptional activity by targeting the protein for proteolysis and inhibiting binding to coactivators, respectively.

Thus far, most studies correlating loss of *VHL* function with HIF dysregulation have been conducted in renal tumors and fully transformed cell lines. As cancer development requires multiple genetic lesions, these cells undoubtedly contain a highly abnormal genetic background. Although recent results have shown that *VHL* inactivation is correlated with stimulation of the HIF pathway in early kidney lesions (Mandriota *et al.* 2002). other genetic abnormalities were not examined. Indeed, cytogenetic analysis of renal clear cell carcinomas shows that a majority of these tumors have lost the short arm of chromosome 3 and contain a myriad of structural aberrations and unbalanced translocations (Gunawan *et al.* 2001). Although reintroduction of *VHL* into RCC lines eliminates their tumorigenic phenotype (Gnarra *et al.* 1996; Iliopoulos *et al.* 1996), this occurs within a background of uncharacterized mutations, making it difficult to identify the effects of *VHL* loss alone. Until now, a formal genetic study to assess the tumorigenic effects of *VHL* loss in euploid primary cells has not been performed. Furthermore, although the regulation of HIF activity is believed to be a multi-step process responsive to $O_2$ levels, it is unclear to what degree these events can occur in normoxic conditions. Here, we utilize gene targeting of *Vhl* in mouse embryonic stem (ES) cells to demonstrate that loss of *Vhl* is sufficient to dysregulate HIF degradation, nuclear accumulation, DNA binding activity and downstream target gene activation, conferring a hypoxic phenotype to normoxic $Vhl^{-/-}$ ES cells. Unexpectedly, $Vhl^{-/-}$ teratocarcinomas are smaller by volume and mass compared to $Vhl^{+/-}$ tumors, suggesting that stimulation of the HIF pathway is not sufficient to induce tumor growth and additional genetic changes must occur to facilitate tumorigenesis in the absence of *Vhl*.

## Results

### Generation of $Vhl^{-/-}$ ES cells

Although renal cancer cell lines deficient for pVHL exhibit constitutive expression of HIF target genes under normoxic conditions, loss of *VHL* alone has not been shown to result in complete disruption of HIF regulation and promotion of tumor formation. To examine the precise role of *Vhl* in these processes, we utilized a genetic strategy based on $Vhl^{+/-}$ mouse J1 embryonic stem (ES) cells (Gnarra *et al.* 1997). The recombined locus maintains intact the *Vhl* promoter region, the first 23 codons, and 3′ untranslated region (Fig. 1A). Homozygous $Vhl^{-/-}$ clones were generated from $Vhl^{+/-}$ ES cells by selecting for loss of the remaining wild-type allele with increasing concentrations of G418 (Mortensen *et al.* 1992). Approximately 200 clones were screened for loss of heterozygosity by Southern blot and/or PCR assays (Figs. 1B and C). Three independently derived $Vhl^{-/-}$ clones were identified, none of which expressed detectable amounts of pVHL when compared to $Vhl^{+/+}$ and $Vhl^{+/-}$ ES cells (Fig. 1D), and these were further assayed for HIF function.

### HIF is constitutively stabilized and maintains DNA binding activity in the absence of *Vhl*

We first investigated the stabilization of HIF-α proteins by western blot and electrophoretic mobility shift assay (EMSA). Immunoblots of nuclear extracts demonstrated that $Vhl^{+/+}$ and $Vhl^{+/-}$ ES cells express low levels of HIF-1α and HIF-2α at 21% $O_2$ (normoxia) (Fig. 2A), which increased dramatically at 1.5% $O_2$ (hypoxia). In contrast, $Vhl^{-/-}$ cells accumulated high levels of HIF-1α and HIF-2α under normoxia. Moreover, HIF-1α and HIF-2α protein levels remained largely unchanged within normoxic and hypoxic extracts when normalized to the Rad50 loading control. The constitutive stabilization of HIF-α subunits in $Vhl^{-/-}$ cells is consistent with data reported for RCC lines (Maxwell *et al.* 1999; Krieg *et al.* 2000).

The nuclear translocation of HTF-α subunits has been reported to be an $O_2$-regulated step, independent of pVHL function (Tanimoto *et al.* 2000). To detect the localization of constitutively stabilized HIF-1α in $Vhl^{-/-}$ cells, western blots were performed using cytoplasmic and nuclear fractions of extracted proteins (Fig. 2B). In $Vhl^{+/+}$ and $Vhl^{+/-}$ cells, stabilized HIF-lα was exclusively detected in the nuclear fraction of hypoxic extracts (Fig. 2B). All $Vhl^{-/-}$ clones exhibited exclusively nuclear accumulation of HIF-1 α under normoxia and hypoxia. Introduction of hemagglutin-tagged (HA)-VHL into clone $Vhl^{-/-.1}$ restored the hypoxic regulation of HIF-lα, consistent with previously reported data (Maxwell *et al.* 1999; Krieg *et al.* 2000). This “rescued” $Vhl^{-/-}$ clone expressed levels of pVHL comparable to RCC lines rescued with HA-VHL (data not shown) (Iliopoulos *et al.* 1996).

HIF DNA binding activity in normoxic and hypoxic $Vhl^{-/-}$ES cells was assessed by EMSA. $Vhl^{+/-}$ ES cells exhibited hypoxic induction of a DNA complex confirmed to be HIF by “supershifting” with an α-ARNT antibody (Fig. 2C, lanes 2 and 3). In contrast, high levels of HIF were detected in normoxic $Vhl^{-/-}$ ES cells (see lanes 4, 7, and 10), which was also by supershifted with the ARNT antibody (lanes 6,9, and 12). We conclude from these results that HIF-α stabilization, subcellular localization, and DNA binding activity are dependent upon the presence of functional pVHL regardless of $O_2$ concentration.

### Loss of *Vhl* is sufficient to activate HIF-mediated transcription under normoxia

To assess the transcriptional activity of HIF in $Vhl^{-/-}$ ES cells, reporter assays using hypoxia response element (HRE)-driven luciferase constructs were performed (Fig. 3A). Normoxic $Vhl^{+/+}$ and $Vhl^{+/-}$ ES cells demonstrated low levels of HIF transcriptional activity induced more than 10-fold by hypoxia. In contrast, although the levels of HIF activity varied between $Vhl^{-/-}$ clones within these assays, the trend consistently showed high levels of HIF activity under normoxic conditions, which were only slightly elevated by hypoxia. Use of a mutant HRE construct, which contains three base pair substitutions to disrupt HIF binding, ablated the hypoxic induction of transcriptional activity in all cell lines demonstrating its HIF-dependence. Furthermore, *Hif-1*$\alpha^{-/-}$ ES cells exhibited reduced levels of luciferase activity in both normoxic and hypoxic conditions, comparable to levels detected using the mutant HRE construct. Importantly, cotransfection of a plasmid encoding HA-VHL with HRE-reporter constructs repressed normoxic HIF activity and restored hypoxic induction of HRE-dependent transcription in $Vhl^{-/-}$ cells (Fig. 3B).

To further investigate the function of stabilized HIF in *Vhl*$^{-/-}$ cells, the activation of endogenous HIF target genes was examined. mRNA expression analysis of several known hypoxia responsive genes (*Glut-1, Vegf, Pgk, Alda* and *Bnip3)* revealed low levels of expression in normoxic *Vhl*$^{+/+}$ and *Vhl*$^{+/-}$ ES cells, which were markedly induced by hypoxia (Fig. 4A). In direct contrast, the expression of HIF target genes in multiple normoxic *Vhl*$^{-/-}$ ES clones was comparable to, if not greater than, their expression in hypoxic in *Vhl*$^{+/+}$ and *Vhl*$^{+/-}$ ES cells. Consistent with reporter gene data, HIF target gene expression remained high and was not greatly affected by hypoxia in two *Vhl*$^{-/-}$ ES clones. Clone *Vhl*$^{-/-.3}$ exhibited high levels of HIF target gene expression under normoxia that was moderately induced by hypoxia, albeit to a lesser degree than wild-type controls. This could be simply a result of clonal variation, as extensive genotyping indicated the absence of contaminating *Vhl*$^{+/-}$ cells in this clone. In all other assays that analyzed HIF target gene activation, *Vhl*$^{-/-.3}$ behaved similarly to the other clones. The expression of all target genes was primarily regulated by HIF, as shown by their greatly reduced expression in *Hif-1*$\alpha^{-/-}$ *ES* cells. However, *Glut-1* and *Vegf* transcripts can be stabilized by hypoxia independently of HIF (Ikeda *et al.* 1995; Levy *et al.* 1996; Levy *et al.* 1996), which may account for the residual hypoxic induction of these genes in *Hif-1*$\alpha^{-/-}$ ES cells.

To further assess the activation of HIF targets, VEGF secretion was measured by ELISA (Fig. 4B). Although the absolute amounts of VEGF secretion varied between all clones, the pattern of *Vegf* regulation observed by Northern blot was recapitulated. VEGF secretion by *Vhl*$^{+/+}$ and *Vhl*$^{+/-}$ cells was substantially induced by hypoxia, while secretion by *Vhl*$^{-/-}$ cells under the same conditions remained similar to their normoxic levels. The induction of VEGF secretion by hypoxia could be restored by reintroduction of HA-VHL into clone *Vhl*$^{-/-.1}$.

When $O_2$ is limiting, cells switch from oxidative phosphorylation to glycolysis as the primary generator of ATP (Pasteur effect). Since the constitutive stabilization of HIF in *Vhl*$^{-/-}$ cells mimicked a hypoxic state, the glycolytic rate of and lactic acid production by these cells was measured. Consistent with their upregulation of glycolytic genes (*Glut-1*, *Pgk*, and *Aldd*), *Vhl*$^{-/-}$ cells consumed more glucose than *Vhl*$^{+/+}$and *Vhl*$^{+/-}$ cells over the course of a one-hour normoxic incubation (Fig. 4C). The higher glycolytic rate of *Vhl*$^{-/-}$ES cells resulted in a substantially increased rate of lactate production over the course of 24 hours, when compared to *Vhl*$^{+/+}$ and *Vhl*$^{+/-}$ cells (Fig. 4D). The increased glycolytic rate in and lactate production by *Vhl*$^{-/-.1}$ was suppressed by reintroduction of HA-VHL, demonstrating that these effects on glycolysis are pVHL-dependent. Therefore, by the criteria of stabilization, nuclear localization, DNA binding activity, target gene activation, and cellular metabolism, loss of *Vhl* alone is sufficient to constitutively activate HIF to hypoxic levels, independent of $O_2$ signaling.

## Loss of *Vhl* does not promote tumor growth

To investigate whether loss of *Vhl* can enhance the tumorigenic potential of ES cells, subcutaneous tumors were generated by injecting *Vhl*$^{+/-}$ and *Vhl*$^{-/-}$ ES cells into the dorsal region of NIH-III immunodeficient mice. Clones *Vhl*$^{-/-.1}$ and *Vhl*$^{-/-.2}$ were used because of their high levels of VEGF secretion relative to *Vhl*$^{+/-}$ cells (Fig. 4B). Surprisingly, *Vhl*$^{-/-}$

tumors were considerably smaller than *Vhl*$^{+/-}$ tumors after 21 or 28 days. Table 1 shows the results of four separate experiments in which *Vhl*$^{-/-}$ tumors were on average 42-68% smaller than *Vhl*$^{+/-}$ tumors. *Vhl*$^{-/-.1}$ tumors grew more slowly than *Vhl*$^{+/-}$controls as measured by tumor volume, contrary to the findings of pVHL-deficient RCC-derived tumors (Fig. 6B) (Iliopoulos *et al.* 1995). Figure 5C shows pooled data from three separate teratocarcinoma experiments at 21 days, in which the masses of tumors formed by clones *Vhl*$^{-/-.1}$ and *Vhl*$^{-/-.2}$ were combined for an n-value of 20. The difference between the masses of *Vhl*$^{+/-}$ and *Vhl*$^{-/-}$ tumors was statistically significant (p= 0.003 by Student t-test). Most importantly, the growth of genetically rescued *Vhl*$^{-/-.1}$ + HA-VHL tumors was similar to *Vhl*$^{+/-}$ controls, demonstrating that this deficiency is functionally dependent upon *Vhl* (Fig 5C).

## Microvessel density is increased in *Vhl*$^{-/-}$ tumors

Gross morphological analysis revealed a higher incidence of hemorrhagic regions within *Vhl*$^{-/-}$ tumors (Figures 6A and B). In addition, primitive tissues derived from all three germ layers were present in *Vhl*$^{-/-}$ tumors, however, more differentiated tissue types such as skeletal muscle, cartilage, neuronal axons, adipocytes and secretory glands were absent or extremely rare, compared to *Vhl*$^{+/-}$ tumors (data not shown). The presence of a subset of these tissues was restored in *Vhl*$^{-/-.1}$ + HA-VHL tumors (data not shown). The ability of *Vhl*$^{-/-}$ ES cells to deposit fibronectin in the extracellular matrix was assessed by immunohistochemistry. *Vhl*$^{+/-}$ tumors exhibited abundant fibronectin staining in the basement membrane of blood vessel endothelial cells (Fig. 6C). Fibronectin staining within *Vhl*$^{-/-}$ tumors was greatly reduced in this cell type (Fig, 6D), consistent with previously reported data for RCCs and *Vhl*$^{-/-}$ embryos (Ohh *et al.* 1998; Hoffman *et al.* 2001). Histological staining for an endothelial cell-specific antigen (CD34) to demarcate tumor vasculature indicated an increase in microvessel density of *Vhl*$^{-/-}$ tumors (47.5 microvessels/mm$^2$ ± 5.0) when compared to *Vhl*$^{+/-}$ tumors (23.1 microvessels/mm$^2$± 3.1) (Figures 6E and F). This statistically significant difference correlated with increased VEGF secretion by *Vhl*$^{-/-}$ cells *in vitro* and is consistent with data reported for RCC-derived tumors (Kondo *et al.* 2002), (p=0.0256 by Student t-test) (Fig 6G). When compared to controls, the phenotype of V*hl*$^{-/-}$ teratocarcinomas paralleled that of *VHL*$^{-/-}$RCCs in terms of fibronectin deposition and microvessel density. However pVHL-deficient teratocarcinomas are smaller than controls, emphasizing a discontinuity between angiogenesis and tumor proliferation.

## *Vhl*$^{-/-}$ tumors are deficient in proliferation but do not exhibit an increase in apoptosis

A possible mechanism for the reduction in tumor volume and mass could be a decrease in cell growth or an increase in cell death. Although undifferentiated *Vhl*$^{-/-}$ cells do not exhibit these defects *in vitro* (data not shown), growth in an *in vivo* tumor microenvironment might reveal such a phenotype. Teratocarcinoma sections were therefore assessed for expression of cell cycle markers. Immunostaining for the proliferation marker Ki-67 (present in the nuclei of all cells not in GO) revealed highly proliferating regions in *Vhl*$^{+/-}$ tumors, most notably in ectoderm-derived tissue (Fig. 7A). Examination of similar tissue types within *Vhl*$^{-/-}$ tumors also revealed Ki-67 positive staining, but at lower levels (Fig. 7B). Morphometric analysis of these regions revealed that 41.5% of cells within *Vhl*$^{-/-}$ tumors were Ki-67$^+$ as compared to 68.1% in *Vhl*$^{+/-}$ tumors and 60.2% in the genetically rescued tumors *Vhl*$^{-/-.1}$ + HA-VHL (Fig 7C), a statistically significant difference (p=0.0028 by Student t-test). This reduction in

proliferation rate, although modest, may account for the slower growth rate of *Vhl*$^{-/-}$ tumors over the course of 21 days.

A concomitant increase in the rate of apoptosis could also cause the reduced mass of *Vhl*$^{-/-}$ teratocarcinomas. To assess this possibility, sections were stained for the apoptotic marker cleaved caspase-3. Although *Vhl*$^{-/-}$ tumors were significantly smaller than *Vhl*$^{+/-}$ tumors, there was no corresponding increase in apoptosis outside of necrotic regions (Figures 7D and E). Morphometric analysis did not reveal any differences between the number of cleaved caspase-3$^{+}$ cells in *Vhl*$^{-/-}$ and *Vhl*$^{+/-}$ sections (2.56% and 2.97% respectively) (Fig. 7F). In addition, apoptosis assessed by TUNEL staining (Figures 7G and H), did not reveal any quantitative differences between *Vhl*$^{-/-}$ and *Vhl*$^{+/-}$tumors, (4.67% and 4.47% respectively), when normalized to DAPI stained nuclei (Figures 7I-K). Although the percentage of TUNEL$^{+}$ cells was greater than that of cleaved caspase-3$^{+}$ cells, both apoptosis detection methods revealed no significant differences between the tumor types. We conclude that although loss of *Vhl* is sufficient to dysregulate HIF, this alone does not promote teratocarcinoma growth in a subcutaneous tumor model. To the contrary, loss of *Vhl* seems to impair the growth of primary cells *in vivo*.

## Discussion

Loss of the tumor suppressor *VHL* is correlated with the development of highly vascularized tumors within the kidney, central nervous system, and retina (Maher and Kaelin 1997). Insight into *VHL*'s role as a tumor suppressor can be found in its ability to bind and target HIF-α subunits for ubiquitin-mediated degradation (Maxwell *et al.* 1999; Cockman *et al.* 2000; Tanimoto *et al.* 2000). We have shown that whereas loss of *Vhl* is sufficient to completely dysregulate HIF, it does not enhance the growth of subcutaneous tumors derived from primary cells. In contrast, *VHL*$^{-/-}$ RCC cells produce rapidly growing xenografts in nude mice, the growth of which is suppressed by reintroduction of functional pVHL. The combined effects of pVHL deficiency and additional mutations within the RCC cells may explain this apparent discrepancy.

The activation of HIF is thought to be an $O_2$-regulated, multi-step pathway requiring α-subunit stabilization, nuclear translocation and recruitment of coactivators (Jiang *et al.* 1997; Pugh *et al.* 1997; Kallio *et al.* 1999; Tanimoto *et al.* 2000; Lando *et al.* 2002). Recent evidence also suggests that full activation of HIF is not only dependent upon inhibition of HIF-α prolyl hydroxylation but also asparagyl hydroxylation within the C-terminal activation domain (CAD) (Lando *et al.* 2002; Sang *et al.* 2002). In our studies, normoxic *Vhl*$^{-/-}$ ES cells displayed constitutive HIF-α stability and HIF activity, neither of which were substantially induced by hypoxia. The nuclear accumulation of stabilized HIF-1α seen in *Vhl*$^{-/-}$ cells is consistent with a recent report suggesting that HIF-1α nuclear export is pVHL-dependent (Groulx and Lee 2002). Constitutively stabilized HIF-1α in *Vhl*$^{-/-}$ cells maintained DNA binding activity and maximally stimulated the expression of downstream target genes. Proper HIF regulation was restored by genetic rescue with HA-VHL. Hence, loss of *Vhl* leads to the full activation of HIF in ES cells, even in the absence of additional hypoxic signaling.

Reintroduction of wild-type *VHL* suppresses the growth of pVHL deficient RCC tumors in nude mice (Gnarra *et al.* 1996; Iliopoulos *et al.* 1996). In contrast, expression of pVHL containing β-domain mutations that disrupt pVHL/HIF-α interaction do not suppress tumor formation, highlighting the importance of HIF regulation for the tumor suppressor function of *VHL* (Bonicalzi *et al.* 2001). pVHL-rescued RCC cells expressing constitutively stabilized HIF-1α produce smaller tumors than those derived from the parental RCC cell line, indicating that loss of *VHL* contributes to tumor growth through HIF-1α-independent mechanisms (Maranchie *et al.* 2002). Interestingly, HlF-2α is more frequently upregulated than HIF-1α in renal clear cell carcinomas (Turner *et al.* 2002) and has been implicated as a critical target for *VHL*-mediated tumor suppression in renal clear cell carcinomas. Our results suggest that constitutive activation of HIF transcriptional activity in *Vhl*$^{-/-}$ ES cell-derived teratocarcinomas promotes tumor angiogenesis, but is itself insufficient to increase tumor growth. This may reflect the fact that our targeted *Vhl*$^{-/-}$ ES cells differ fundamentally from pVHL-deficient RCC cell lines in at least one important way; specifically, they have not undergone selection *in vivo* for the ability to overcome proliferation checkpoints and apoptotic controls known to suppress tumorigenesis. The chromosomal abnormalities observed in RCC cell lines, (Gunawan *et al.* 2001), are consistent with the idea that genetic instability underlies the multiple genetic hits that facilitate tumor formation (Hanahan and Weinberg 2000). In contrast, the use of *Vhl*$^{-/-}$ ES cells permits assessment of pVHL function in an intact genetic background. Taken together, these results suggest that the tumorigenic phenotype of RCC cell lines requires not only pVHL's HIF-dependent and HIF-independent functions, but also other oncogenic mutations.

The precise role of HIF in tumor development is controversial due to the conflicting results of several tumor models. While one group found that genetic disruption of the *Hif-1*α locus results in the accelerated growth of poorly vascularized *Hif-1*α$^{-/-}$ teratocarcinomas (Carmeliet *et al.* 1998), others have shown that the absence of HIF activity in teratocarcinomas and fibrosarcomas impairs tumor growth, but not tumor angiogenesis (Ryan *et al.* 1998; Ryan *et al.* 2000; Hopfl *et al.* 2002). Additional support for HIF as a positive regulator of tumor growth has been obtained from tumor models using non-primary cells. In three different tumor cell lines, loss or disruption of HIF activity also inhibits expression of HIF target genes, tumor vasculature and growth (Maxwell *et al.* 1997; Kung *et al.* 2000; Hopfl *et al.* 2002). Disrupted binding of HIF to coactivators p300 and CBP can also attenuate tumor growth (Kung *et al.* 2000). Therefore, the full oncogenic consequences of HIF dysregulation are still unresolved and will probably depend considerably on genetic background.

The meager growth of *Vhl*$^{-/-}$ teratocarcinomas, a rather unexpected phenotype considering *VHL*'s role as a tumor suppressor, did not result from increased apoptosis in *Vhl*$^{-/-}$ ES cell-derived tumors. This point was of particular interest, as the proapoptotic gene *Bnip-3* has recently been described as a novel HIF transcriptional target (Bruick 2000; Sowter *et al.* 2001). In fact, *Bnip-3* expression has been shown to be stimulated in hypoxic regions of human tumors (Sowter *et al.* 2001). Although the mRNA transcript of *Bnip-3* was highly expressed in both normoxic and hypoxic *Vhl*$^{-/-}$ cell (Fig 4A), this did not equate with an increase in cell death or a growth disadvantage *in vitro*. In fact, doubling Lime and S phase

composition as measured by propidium iodide incorporation of *Vhl*$^{-/-}$ cells, did not differ significantly from *Vhl*$^{+/+}$ or *Vhl*$^{+/-}$ cells (data not shown). Furthermore, cleaved caspase-3 and TUNEL staining did not reveal an increase in apoptosis in *Vhl*$^{-/-}$ teratocarcinomas (Figures 7D-I). These results suggest that the expression of *Bnip-3* in undifferentiated and differentiated ES cells does not induce apoptosis.

*Vhl*'s effects on early development and tumor growth are contrary to those found for other tumor suppressors such as PTEN. Loss of PTEN also results in embryonic lethality, but still enhances the growth of tumors derived from primary ES cells and embryonic fibroblasts (Di Cristofano *et al.* 1998; Stiles *et al.* 2002), The aberrant differentiation of *Pten*$^{-/-}$ cells, although detrimental to early development, is actually beneficial for tumor proliferation. In contrast, loss of *VHL* may only be able to induce tumor growth in a background of genetic changes. Cytogenetic abnormalities have been observed in RCC cells, and a minority of RCCs and RCC-derived cell lines have been shown to harbor p53 mutations (Reiter *et al.* 1993). Amplifications of the oncogenes c-myc and K-ras may also play a role in the generation of renal clear cell carcinomas (Kozma *et al.* 1997).

It is important to note that our teratocarcinoma model does not recreate the selective pressures that generate pVHL-deficient human cancers. In many ways, the development of heterogeneous tissues within teratocarcinomas reflects the differentiation of ES cells in early embryogenesis. Loss of *Vhl* in early development results in growth retarded embryos, which die between days E10.5-12.5 (Gnarra *et al.* 1997). *Vhl*$^{-/-}$teratocarcinomas, although less proliferative, appear to contain more primitive tissue types when compared to controls (data not shown). The decreased growth and differentiation of *Vhl*$^{-/-}$ teratocarcinomas suggests that pVHL may be required for the proliferation and/or initial differentiation of primary cells. For example, recent studies from our lab indicate that *Vhl*$^{-/-}$ ES cells generate reduced numbers of hematopoietic progenitors in *in vitro* assays (F.A.M. and M.C.S., unpublished). In conclusion, our data suggest that although inactivation of *VHL*'s tumor suppressor functions can contribute to the malignancy of renal cancer, disruption of these same pathways in pluripotent cells appears to be detrimental to their growth and/or differentiation.

## Experimental Procedures

### Generation and Genotyping of Vhl$^{+/-}$ ES cells

$5.0 \times 10^4$ *Vhl*$^{+/-}$ ES cells were plated on 10cm gelatin-coated tissue culture dishes in media containing 4.0mg/ml of G418, to promote loss of the second wild-type *Vhl* allele. Resistant clones were isolated and expanded after 6-7 days of selection. Genomic DNA extracted from cultured ES cells was digested with HindIII for Southern blot analysis using a probe generated from an AccI/XbaI fragment from the *Vhl* 3′ UTR. PCR was also used to genotype ES clones. Oligonucleotide primers included those specific for wild-type *Vhl* exon 3, 5′-ACT GAA AAC GTC TTC CTC CCT CGG G(reverse) and wild-type exon 1, 5′-GCG GAA GGA CAT ACA GCG ACT GAG CC-3′(forward) and internal neo sequence 5′-TGA CTA GGG GAG GAG TAG AAG GTG GCG-3′ (reverse).

### Generation of "rescued" ES cell lines

Wild-type human cDNA encoding pVHL with an N-terminal hemagglutin epitope tag (HA-VHL) was obtained as a generous gift from Dr. W. Kaelin. $2x10^7$ *Vhl*$^{-/-.1}$ ES cells were elcctroporated with 20μg pf PvuII linearized expression construct Station II containing HA-VHL with an SV-40 polyadenylation sequence at the C-terminus. Resistant clones were screened by Southern blot using a 900bp probe generated from a HindIII-EcoRI fragment from HA-tagged VHL cDNA. Clones with evidence of an integration event were further analyzed by Western blot.

### Western Blot Analysis

For all Western blot and EMSA analyses, 6-7 × $10^6$ cells were plated on 10 cm gelatin coated tissue culture dishes such that the density of the cells at the time of lysis was ∼60-70% confluent. Hypoxia, defined as 1.5% $O_2$, was generated using an In $Vivo_2$ hypoxic workstation (Ruskinn Technologies, Leeds, UK) for Western and EMSA analyses, or an IG750 variable $O_2$ tissue culture incubator (Jouan Inc.) for reporter and Northern analyses.

Whole cell protein lysates were prepared using WCE buffer: 150mM NaCl, 50mM Tris, pH 7.4, 5mM EDTA, 0.1% SDS, and Complete Protease Inhibitor (Roche Molecular Biochemicals). Nuclear and cytoplasmic fractions of protein extracts were prepared using a modified Dignam protocol (Maltepe *et al.* 2000) with Buffer A further modified to contain 0.1% NP-40 and Buffer C containing 300mM NaCl. For hypoxic extracts, cells were manipulated inside a hypoxic chamber using phosphate-buffered saline and Buffer A that had been equilibrated to the hypoxic environment. Extracts were electrophoresed, transferred, and immunoblotted according to standard protocols using 5% non-fat dry milk (Carnation) in Tris-buffered saline/Tween 20, as a blocking agent. Blots were stained with Ponceau S to ensure equal loading. Antibodies used include: α-mouse pVHL (Santa Cruz), α- human pVHL (Pharmingen), α- mouse HIF-1α and HIF-2α (Novus), α-mouse Rad-50 (Transduction Laboratories) and α-mouse β-Tubulin (InnoGenex). Horseradish peroxidase-conjugated α-rabbit and α-mouse secondary antibodies were purchased from Cell Signaling Technologies and used at dilutions of 1:2000. ECL reagents were purchased from Amersham Biosciences. Blots were stripped in 61.5mM Tris (pH 6.8), 2% SDS and 100mM β-mercaptoethanol at 55°C for 1 h before being blocked and re-probed.

### Electrophoretic mobility shift assay (EMSA)

EMSA analyses have been previously described (Maltepe *et al.* 2000). In brief, 5 μg of nuclear extracts were incubated in binding buffer consisting of 10mM Tris-HCl (pH 7.5), 50mM NaCl, 50mM KC1, 1mM MgC12, 5mM dithiothreitol, 1mM EDTA, and 5% glycerol to which 0.05 mg/ml bovine serum albumin, 0.025μg/ml of CREB oligo, and $10^6$ dpm of labeled probe and where indicated 0.5μ1 of polyclonal α-ARNT antiserum (Novus) were added. The 24-bp oligonucleotide probe was derived from the erythropoietin HRE, 5′-GCC CTA CGT GCT GTC CTC A3′.

### Reporter Assays

The HRE-luciferase reporter constructs were previously described (Arsham *et al.* 2002). Transfection efficiency was assessed by cotransfection of a renilla luciferase gene under the control of a minimal tyrosine kinase promoter. Where indicated, cells were also cotransfected with plasmid encoding HA- tagged full-length human pVHL. For transient tansfections, $2x10^6$ ES cells were plated on gelatin treated 6-well plates and allowed to recover overnight. Cells were transfected the next morning using Lipofectamine Plus reagent (Gibco BRL) according to manufacturers protocol. Cells were transfected for 4hrs and one half of each sample was exposed to hypoxia for 18hrs. Proteins were extracted from samples using reporter lysis buffer and dual luciferase assays were performed according to manufacturer's guidelines (Promega).

### Northern Analysis

For Northern blots, $2\text{-}3 \times 10^6$ cells/ 10cm tissue culture dish were plated and allowed to recover overnight. Where indicated, cells were incubated in hypoxia for 18hrs. All cells were lysed in Trizol (InVitrogen) according to manufacturer's instructions in ambient air. 20μg of total RNA were electrophoresed in 1.5% denaturing (formaldehyde) agarose gels and transferred to Hybond N+ membranes (Amersham). Murine *Vegf*, *Pgk*, *Alda*, and *Glut-1* probes have been previously described (Maltepe *et al.* 1997). Murine *Bnip3* probe was generated by RT-PCR from cDNA synthesized from murine FL5.12 cell RNA. A 738bp fragment was amplified between bp11 and 749 using primers 5′TGC CCC TGC TAC CTC TCG (forward) and 5′ CAT AGT GCA AAC ACC CAA GG (reverse). PCR products were sequenced and confirmed to be identical to GenBank sequence NM_009760 for murine *Bnip3*.

### VEGF ELISA

VEGF quantitation was performed using the Quantikine M Murine Immunoassay kit, (R&D Systems) according to manufacturers protocol. $7.5x10^5$ cells were seeded on gelatin coated 12-well plates and incubated in hypoxia for 18hrs where indicated. Conditioned medium was incubated with a mouse specific VEGF polyclonal antibody bound to a microtiter plate. After several washes, a second enzyme-linked polyclonal antibody specific for mouse VEGF was added. Sample values were obtained according to manufacturers protocol. Recorded values were normalized for cell number.

### Glycolytic Rate Assay

Glycolysis was assayed as the rate of conversion of $^3$H-Glucose to $^3H_20$ as previously described (Liang *et al.* 1997). $1x10^6$ cells were washed once in PBS and media was replaced with 0.5ml of Krebs buffer and incubated for 30min at 37°C. Krebs buffer was then replaced with 0.5 ml of Krebs buffer containing 10mM glucose and spiked with 10μCi of 5-$^3$H-glucose. Following incubation for 1h at 37°C, triplicate 50μl aliquots were transferred to uncapped PCR tubes containing 50μ1 of 0.2N HC1, and these tubes were transferred to scintillation vials containing 0.5ml of $H_2O$ such that the water in the vial and the contents of the PCR tubes were not allowed to mix. The vials were sealed, and diffusion was allowed to occur for 48hrs. The amounts of diffused and undiffused $^3$H were determined by scintillation

counting. Appropriate $^{3}$H-glucose-only and $^{3}H_2O$-only controls were included, enabling the calculation of $^{3}H_2O$ in each sample and thus the rate of glycolysis.

### Lactate Secretion Assay

Lactate concentrations were indirectly determined by a colorimetric assay, which converts the lactic acid present in the media into $H_2O_2$, resulting in the oxidative condensation of a chromogen precursor (Sigma). Approximately $5x10^4$ cells were plated on gelatin coated 24-well plates and allowed to recover overnight. Samples were collected and individual cell counts were obtained every 24hrs for two days thereafter

### Mouse teratocarcinoma assay

$5x10^6$ cells were suspended in 100μl of Phosphate-Buffered Saline (Gibco) and injected subcutaneously into the dorsal area of 4-6 week old female NIH-III immunodeficient mice (Taconic). After 7 days tumors were measured every 2-3 days with calipers in the two greatest dimensions to calculate tumor volume. After 21 or 28 days, tumors were excised, photographed, weighed, frozen for protein assays and fixed in 4% paraformaldehyde.

### Immunohistochemistry

Tumor samples were fixed in 4% paraformaldehyde and paraffin embedded by standard techniques. 6μm sections of each sample were incubated overnight with antibodies generated against fibronectin (BD Scientific), cleaved caspase-3 (Calbiochem), Ki-67 (Novacastra), and CD-34 (BD Scientific). A TUNEL assay, *In Situ* Cell Death Detection Kit, was utilized according to the manufacturers protocol (Roche). α-mouse and α-rat secondary antibodies were biotinylated and staining achieved by a strepavidin-biotin system conjugated with horseradish peroxidase (Vector Lab). Fibronectin, CD-34, and active caspase-3 photographs were taken with a Nikon N6006 35mm camera. Ki-67 photographs were taken with a Spot RT slider digital camera (Diagnostic Instruments Inc.) with a magnification of 0.76X. Morphometric analysis was performed on three to five randomly chosen sections of each tumor using the analytical program Image Pro (Phase 3 Imaging). The number of positive cells was calculated as the total area of positive staining divided by the area of an individual positive cell. The percentage positive cells were calculated as the number of positive cells divided by the total number of cells.

## Acknowledgments

We thank Min-min Lu, Q.C. Yu, Cynthia Clendenin, Clint Culpepper, Frank Winslow, Marian Harris, J Thompson, and Nathalie Innocent for reagents and technical assistance. This research was supported by National Institute of Health Grants HL63310 (M.C.S.) and 1F31HD (F.A.M.) and the Abramson Family Cancer Research Institute. M.C.S. is an investigator at the Howard Hughes Institute.

## References

Arany Z, Huang LE, et al. An essential role for p300/CBP in the cellular response to hypoxia. Proc Natl Acad Sci U S A. 1996; 93:12969–73. [PubMed: 8917528]

Arsham AM, Plas DR, et al. Phosphatidylinositol 3-kinase/Akt signaling is neither required for hypoxic stabilization of HIF-1 alpha nor sufficient for HIF-1-dependent target gene transcription. J Biol Chem. 2002; 277:15162–70. [PubMed: 11859074]

Bindra RS, Vasselli JR, et al. VHL-mediated hypoxia regulation of cyclin D1 in renal carcinoma cells. Cancer Res. 2002; 62:3014–9. [PubMed: 12036906]

Bonicalzi ME, Groulx I. Role of exon 2-encoded beta -domain of the von Hippel-Lindau tumor suppressor protein. J Biol Chem. 2001; 276:1407–16. [PubMed: 11024059]

Bruick RK. Expression of the gene encoding the proapoptotic Nip3 protein is induced by hypoxia. Proc Natl Acad Sci U S A. 2000; 97:9082–7. [PubMed: 10922063]

Bruick RK, McKnight SL. A Conserved Family of Prolyl-4-Hydroxylases That Modify HIF. Science. 2001; 11:11.

Carmeliet P, Dor Y, et al. Role of HEF-1alpha in hypoxia-mediated apoptosis, cell proliferation and tumour angiogenesis. Nature. 1998; 394:485–90. [PubMed: 9697772]

Carrero P, Okamoto K, et al. Redox-regulated recruitment of the transcriptional coactivators CREB-binding protein and SRC-1 to hypoxia-inducible factor 1alpha. Mol Cell Biol. 2000; 20:402–15. [PubMed: 10594042]

Cockman ME, Masson N, et al. Hypoxia inducible factor-alpha binding and ubiquitylation by the von Hippel-Lindau tumor suppressor protein. J Biol Chem. 2000; 275:25733–41. [PubMed: 10823831]

Di Cristofano A, Pesce B, et al. Pten is essential for embryonic development and tumour suppression. Nat Genet. 1998; 19:348–55. [PubMed: 9697695]

Ebert BL, Bunn HF. Regulation of transcription by hypoxia requires a multiprotein complex that includes hypoxia-inducible factor 1, an adjacent transcription factor, and p300/CREB binding protein. Mol Cell Biol. 1998; 18:4089–96. [PubMed: 9632793]

Epstein AC, Gleadle JM, et al. C. elegans EGL-9 and Mammalian Homologs Define a Family of Dioxygenases that Regulate HIF by Prolyl Hydroxylation. Cell. 2001; 107:43–54. [PubMed: 11595184]

Foster K, Prowse A, et al. Somatic mutations of the von Hippel-Lindau disease tumour suppressor gene in non-familial clear cell renal carcinoma. Hum Mol Genet. 1994; 3:2169–73. [PubMed: 7881415]

Gnarra JR, Duan DR, et al. Molecular cloning of the von Hippel-Lindau tumor suppressor gene and its role in renal carcinoma. Biochim Biophys Acta. 1996; 1242:201–10. [PubMed: 8603073]

Gnarra JR, Tory K, et al. Mutations of the VHL tumour suppressor gene in renal carcinoma. Nat Genet. 1994; 7:85–90. [PubMed: 7915601]

Gnarra JR, Ward JM, et al. Defective placental vasculogenesis causes embryonic lethality in VHL-deficient mice. Proc Natl Acad Sci U S A. 1997; 94:9102–7. [PubMed: 9256442]

Gnarra JR, Zhou S, et al. Post-transcriptional regulation of vascular endothelial growth factor mRNA by the product of the VHL tumor suppressor gene. Proc Natl Acad Sci U S A. 1996; 93:10589–94. [PubMed: 8855222]

Groulx I, Lee S. Oxygen-dependent ubiquitination and degradation of hypoxia-inducible factor requires nuclear-cytoplasmic trafficking of the von Hippel-Lindau tumor suppressor protein. Mol Cell Biol. 2002; 22:5319–36. [PubMed: 12101228]

Gunawan B, Huber W, et al. Prognostic impacts of cytogenetic findings in clear cell renal cell carcinoma: gain of 5q31-qter predicts a distinct clinical phenotype with favorable prognosis. Cancer Res. 2001; 61:7731–8. [PubMed: 11691785]

Haase VH, Glickman JN, et al. Vascular tumors in livers with targeted inactivation of the von Hippel-Lindau tumor suppressor. Proc Natl Acad Sci U S A. 2001; 98:1583–8. [PubMed: 11171994]

Hanahan D, Weinberg RA. The hallmarks of cancer. Cell. 2000; 100:57–70. [PubMed: 10647931]

Hoffman MA, Ohh M, et al. von Hippel-Lindau protein mutants linked to type 2C VHL disease preserve the ability to downregulate HIF. Hum Mol Genet. 2001; 10:1019–27. [PubMed: 11331612]

Hopfl G, Wenger RH, et al. Rescue of hypoxia-inducible factor-1 alpha-deficient tumor growth by wild-type cells is independent of vascular endothelial growth factor. Cancer Res. 2002; 62:2962–70. [PubMed: 12019179]

Ikeda E, Achen MG, et al. Hypoxia-induced transcriptional activation and increased mRNA stability of vascular endothelial growth factor in C6 glioma cells. J Biol Chem. 1995; 270:19761–6. [PubMed: 7544346]

Iliopoulos O, Kibel A, et al. Tumour suppression by the human von Hippel-Lindau gene product. Nat Med. 1995; 1:822–6. [PubMed: 7585187]

Iliopoulos O, Levy AP, et al. Negative regulation of hypoxia-inducible genes by the von Hippel-Lindau protein. Proc Natl Acad Sci U S A. 1996; 93:10595–9. [PubMed: 8855223]

Ivan M, Kondo K, et al. HIFalpha targeted for VHL-mediated destruction by proline hydroxylation: implications for 02 sensing. Science. 2001; 292:464–8. [PubMed: 11292862]

Jaakkola P, Mole DR, et al. Targeting of HIF-alpha to the von Hippel-Lindau ubiquitylation complex by O2-regulated prolyl hydroxylation. Science. 2001; 292:468–72. [PubMed: 11292861]

Jiang BH, Zheng JZ, et al. Transactivation and inhibitory domains of hypoxia-inducible factor 1alpha. Modulation of transcriptional activity by oxygen tension. J Biol Chem. 1997; 272:19253–60. [PubMed: 9235919]

Kallio PJ, Wilson WJ, et al. Regulation of the hypoxia-inducible transcription factor 1alpha by the ubiquitin-proteasome pathway. J Biol Chem. 1999; 274:6519–25. [PubMed: 10037745]

Kamada M, Suzuki K, et al. von Hippel-Lindau protein promotes the assembly of actin and vinculin and inhibits cell motility. Cancer Res. 2001; 61:4184–9. [PubMed: 11358843]

Kondo K, Klco J, et al. Inhibition of HIF is necessary for tumor suppression by the von Hippel-Lindau protein. Cancer Cell. 2002; 1:237–46. [PubMed: 12086860]

Kozma L, Kiss I. Investigation of c-myc and K-ras amplification in renal clear cell adenocarcinoma. Cancer Lett. 1997; 111:127–31. [PubMed: 9022137]

Krieg M, Haas R, et al. Up-regulation of hypoxia-inducible factors HIF-1alpha and HIF-2alpha under normoxic conditions in renal carcinoma cells by von Hippel-Lindau tumor suppressor gene loss of function. Oncogene. 2000; 19:5435–43. [PubMed: 11114720]

Kung AL, Wang S, et al. Suppression of tumor growth through disruption of hypoxia-inducible transcription. Nat Med. 2000; 6:1335–40. [PubMed: 11100117]

Lando D, Peet DJ, et al. Asparagine hydroxylation of the HIF transactivation domain a hypoxic switch. Science. 2002; 295:858–61. [PubMed: 11823643]

Levy AP, Levy NS, et al. Hypoxia-inducible protein binding to vascular endothelial growth factor mRNA and its modulation by the von Hippel-Lindau protein. J Biol Chem. 1996; 271:25492–7. [PubMed: 8810320]

Levy AP, Levy NS, et al. Post-transcriptional regulation of vascular endothelial growth factor by hypoxia. J Biol Chem. 1996; 271:2746–53. [PubMed: 8576250]

Liang Y, Buettger C, et al. Chronic effect of fatty acids on insulin release is not through the alteration of glucose metabolism in a pancreatic beta-cell line (beta HC9). Diabetologia. 1997; 40:1018–27. [PubMed: 9300238]

Lisztwan J, Imbert G, et al. The von Hippel-Lindau tumor suppressor protein is a component of an E3 ubiquitin-protein ligase activity. Genes Dev. 1999; 13:1822–33. [PubMed: 10421634]

Lonergan KM, Iliopoulos O, et al. Regulation of hypoxia-inducible mRNAs by the von Hippel-Lindau tumor suppressor protein requires binding to complexes containing elongins B/C and Cul2. Mol Cell Biol. 1998; 18:732–41. [PubMed: 9447969]

Maher ER, Kaelin WG Jr. von Hippel-Lindau disease. Medicine (Baltimore). 1997; 76:381–91. [PubMed: 9413424]

Maltepe E, Keith B, et al. The role of ARNT2 in tumor angiogenesis and the neural response to hypoxia. Biochem Biophys Res Commun. 2000; 273:231–8. [PubMed: 10873592]

Maltepe E, Schmidt JV, et al. Abnormal angiogenesis and responses to glucose and oxygen deprivation in mice lacking the protein ARNT. Nature. 1997; 386:403–7. [PubMed: 9121557]

Mandriota SJ, Turner KJ, et al. HIF activation identifies early lesions in VHL kidneys: evidence for site-specific tumor suppressor function in the nephron. Cancer Cell. 2002; 1:459–68. [PubMed: 12124175]

Maranchie JK, Vasselli JR, et al. The contribution of VHL substrate binding and HEF1-alpha to the phenotype of VHL loss in renal cell carcinoma. Cancer Cell. 2002; 1:247–55. [PubMed: 12086861]

Maxwell PH, Dachs GU, et al. Hypoxia-inducible factor-1 modulates gene expression in solid tumors and influences both angiogenesis and tumor growth. Proc Natl Acad Sci U S A. 1997; 94:8104–9. [PubMed: 9223322]

Maxwell PH, Wiesener MS, et al. The tumour suppressor protein VHL targets hypoxia-inducible factors for oxygen-dependent proteolysis. Nature. 1999; 399:271–5. [PubMed: 10353251]

Mortensen RM, Conner DA, et al. Production of homozygous mutant ES cells with a single targeting construct. Mol Cell Biol. 1992; 12:2391–5. [PubMed: 1569957]

Ohh M, Park CW, et al. Ubiquitination of hypoxia-inducible factor requires direct binding to the beta-domain of the von Hippel-Lindau protein. Nat Cell Biol. 2000; 2:423–7. [PubMed: 10878807]

Ohh M, Yauch RL, et al. The von Hippel-Lindau tumor suppressor protein is required for proper assembly of an extracellular fibronectin matrix. Mol Cell. 1998; 1:959–68. [PubMed: 9651579]

Pause A, Lee S, et al. The von Hippel-Lindau tumor suppressor gene is required for cell cycle exit upon serum withdrawal. Proc Natl Acad Sci U S A. 1998; 95:993–8. [PubMed: 9448273]

Pause A, Lee S, et al. The von Hippel-Lindau tumor-suppressor gene product forms a stable complex with human CUL-2, a member of the Cdc53 family of proteins. Proc Natl Acad Sci U S A. 1997; 94:2156–61. [PubMed: 9122164]

Pugh CW, O'Rourke JF, et al. Activation of hypoxia-inducible factor-1; definition of regulatory domains within the alpha subunit. J Biol Chem. 1997; 272:11205–14. [PubMed: 9111021]

Reiter RE, Anglard P, et al. Chromosome 17p deletions and p53 mutations in renal cell carcinoma. Cancer Res. 1993; 53:3092–7. [PubMed: 8319216]

Ryan HE, Lo J, et al. HIF-1a is required for solid tumor formation and embryonic vascularization. EMBO J. 1998; 17:3005–3015. [PubMed: 9606183]

Ryan HE, Poloni M, et al. Hypoxia-inducible factor-1alpha is a positive factor in solid tumor growth. Cancer Res. 2000; 60:4010–5. [PubMed: 10945599]

Sang N, Fang J, et al. Carboxyl-terminal transactivation activity of hypoxia-inducible factor 1 alpha is governed by a von Hippel-Lindau protein-independent, hydroxylation-regulated association with p300/CBP. Mol Cell Biol. 2002; 22:2984–92. [PubMed: 11940656]

Sowter HM, Ratcliffe PJ, et al. HIF-1-dependent regulation of hypoxic induction of the cell death factors BNIP3 and NIX in human tumors. Cancer Res. 2001; 61:6669–73. [PubMed: 11559532]

Stiles B, Gilman V. Essential role of AKT-1/protein kinase B alpha in PTEN-controlled tumorigenesis. Mol Cell Biol. 2002; 22:3842–51. [PubMed: 11997518]

Tanimoto K, Makino Y, et al. Mechanism of regulation of the hypoxia-inducible factor-1 alpha by the von Hippel-Lindau tumor suppressor protein. Embo J. 2000; 19:4298–309. [PubMed: 10944113]

Turner KJ, Moore JW, et al. Expression of hypoxia-inducible factors in human renal cancer: relationship to angiogenesis and to the von Hippel-Lindau gene mutation. Cancer Res. 2002; 62:2957–61. [PubMed: 12019178]

## Significance

Loss of the pVHL tumor suppressor protein is associated with tumors within the CNS, retina and kidney. pVHL targets the α-subunits of Hypoxia Inducible Factor (HIF) for ubiquitin-mediated degradation in an $O_2$-regulated manner. The degree to which constitutive HIF stabilization contributes to *VHL* disease has been studied in tumor-derived cell lines that contain other genetic lesions. We generated primary *Vhl*$^{-/-}$ ES cells which display maximal HIF activity under normoxic conditions. These results contrast published reports indicating that full HIF activity requires multiple pVHL-independent, $O_2$-regulated steps, including nuclear transport and transactivation. Surprisingly, *Vhl*$^{-/-}$ ES cells generate smaller teratocarcinomas than controls, suggesting a growth disadvantage in pVHL-deficient primary cells. Therefore, *VHL*'s tumor suppressor activity may be manifested only in a background of other mutations.

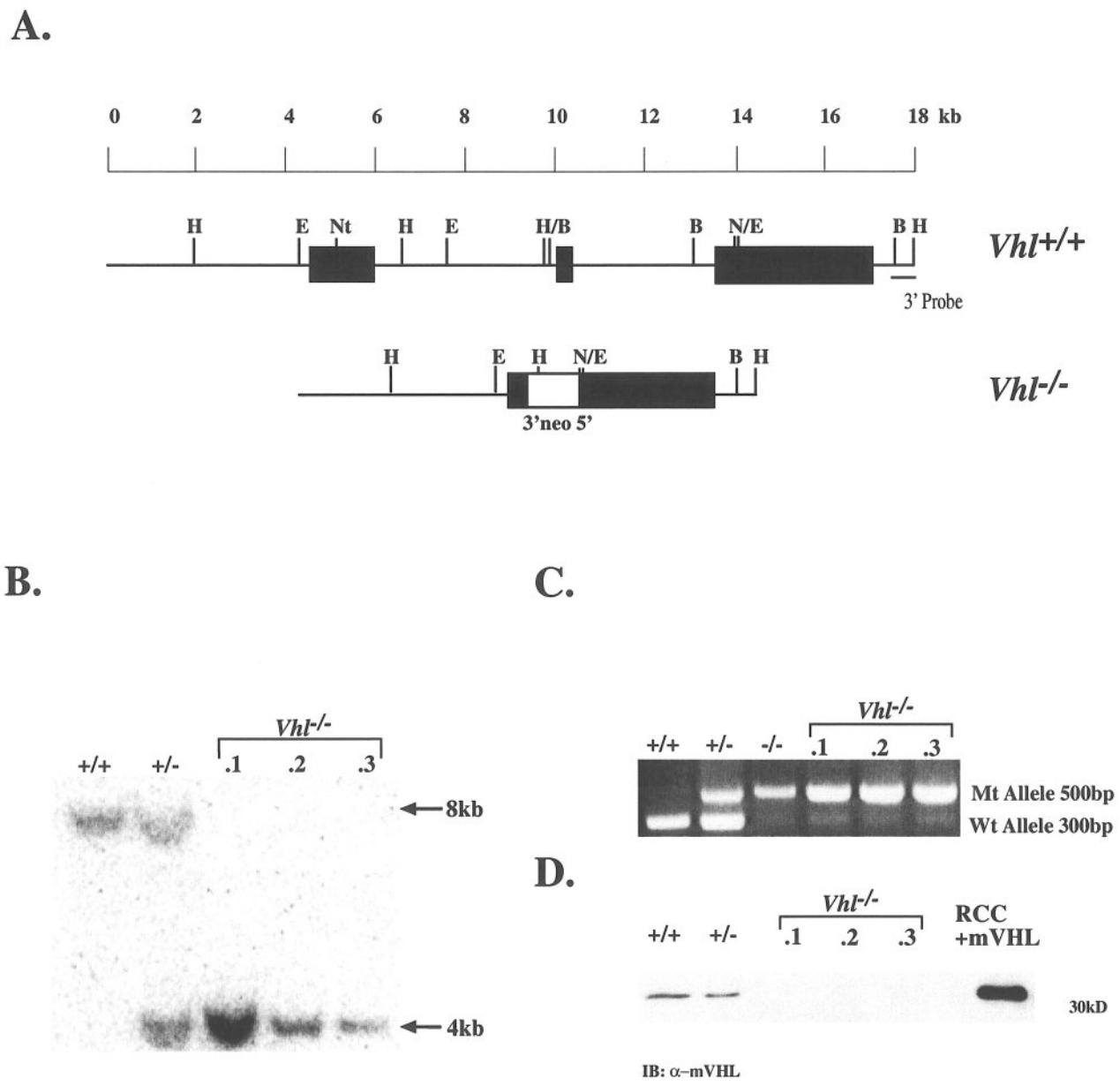


**Figure 1. Generation of *Vhl*$^{-/-}$ ES cells**

A: Filled boxes represent the three *Vhl* exons while the open box depicts the pgk-neo selectable marker within the targeting vector. The 3′ flanking probe used in Southern blots is indicated. B: Detection of wild-type and targeted alleles in ES cells by HindIII digestion and hybridization to the 3′ flanking probe revealed an 8-kb wild-type fragment and 4-kb mutant fragment in *Vhl*$^{+/-}$ and ES clones 1, 2, and 3. C: PCR genotyping of ES clones demonstrated a 300-bp wild-type and a 500-bp mutant product. The lower band visible within lanes 3-6 is a background signal thought not to represent the wild-type allele because of its greater size and decreased intensity. D: Immunoblot for pVHL in ES clones detected a 30kd protein in wild-type and *Vhl*$^{+/-}$ ES cell whole cell extracts but not in clones 1, 2, and 3. A pVHL-

deficient RCC cell line stably transfected with HA-tagged murine pVHL was used as a control.

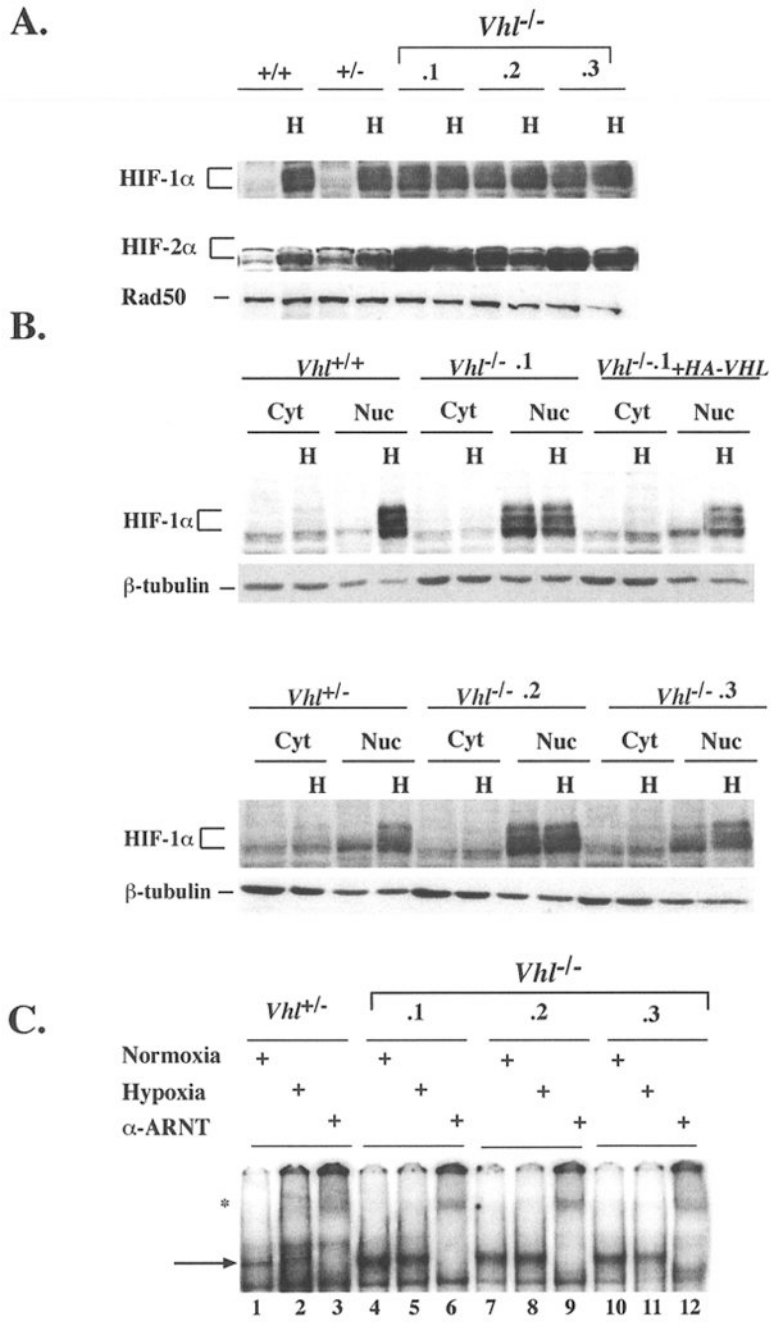


**Figure 2. HTF stabilization and DNA binding activity in the absence of *Vhl***

A: Nuclear extracts were prepared from ES cells cultured under normoxia (21% $O_2$) or hypoxia (1.5% $O_2$) for 4hrs. Low levels of HTF-lα and HIF-2α proteins were present under normoxia and become markedly induced by hypoxia in $Vhl^{+/+}$ and $Vhl^{+/-}$ ES cells. In the absence of *Vhl*, HIF-α proteins became stabilized under normoxia at higher levels than $Vhl^{+/+}$ and $Vhl^{+/-}$ ES cells and were not substantially induced by hypoxia. Nuclear protein Rad50 was utilized as a loading control. B: Immonoblot for HTF-1α in cytoplasmic and nuclear fraction revealed that stabilized HTF-1α accumulated exclusively in the nucleus of

*Vhl*$^{-/-}$ ES cells. HIF-1α regulation was restored by stable transfection of HA-VHL into clone *Vhl*$^{-/-.1}$. Loading control β-tubulin, although more abundant in cytoplasmic fractions, demonstrated equivalent protein amounts were loaded per cell sample. C: EMSA of 5.0μg nuclear extracts prepared from cells grown under normoxic or hypoxic conditions for 4hrs where indicated. HIF DNA binding activity was maintained in *Vhl*$^{-/-}$ cells under normoxia. The arrow represents the HIF/ARNT complex, which was shown to be specific by supershifting with an α-ARNT antibody, marked by an asterisks.

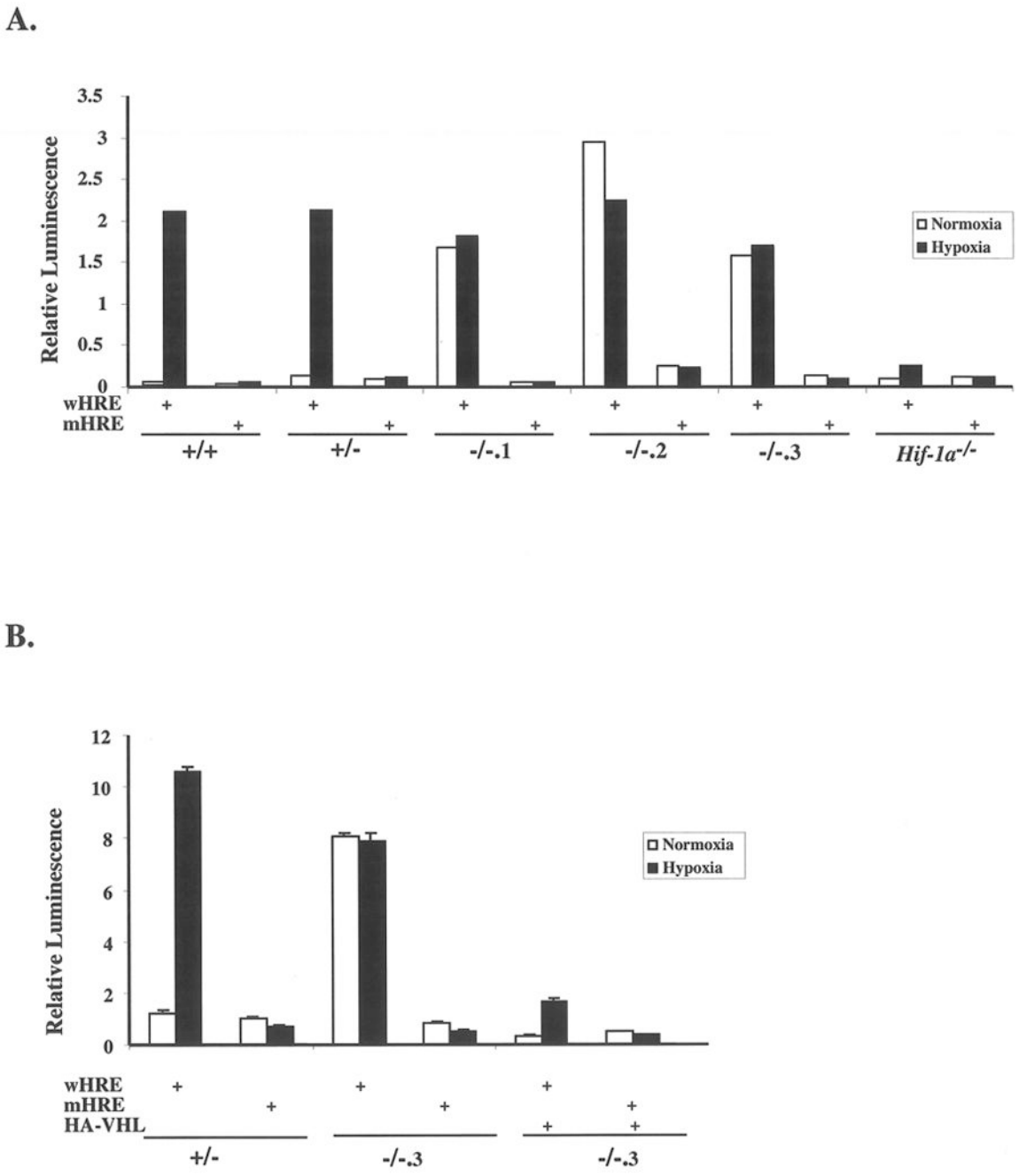


**Figure 3. HIF transcriptional activity is dysregulated in *Vhl*$^{-/-}$ ES cells**

A: ES cells were transiently transfected with wild-type (wHRE) or mutant (mHRE) reporter constructs and transcriptional activity was measured in normoxic (21% $O_2$) or hypoxic (1.5% $O_2$) cells at 16hrs. Luciferase activity detected in normoxic *Vhl*$^{-/-}$ clones was not further induced by hypoxia. Data represents one of three independent assays in which similar results were produced. B: ES cells were cotransfected with wHRE or mHRE plus or minus a plasmid encoding HA-VHL. The presence of HA-VHL decreased the normoxic

levels of HIF activity and restored hypoxic induction. Assays were performed in triplicate and bars represent standard error.

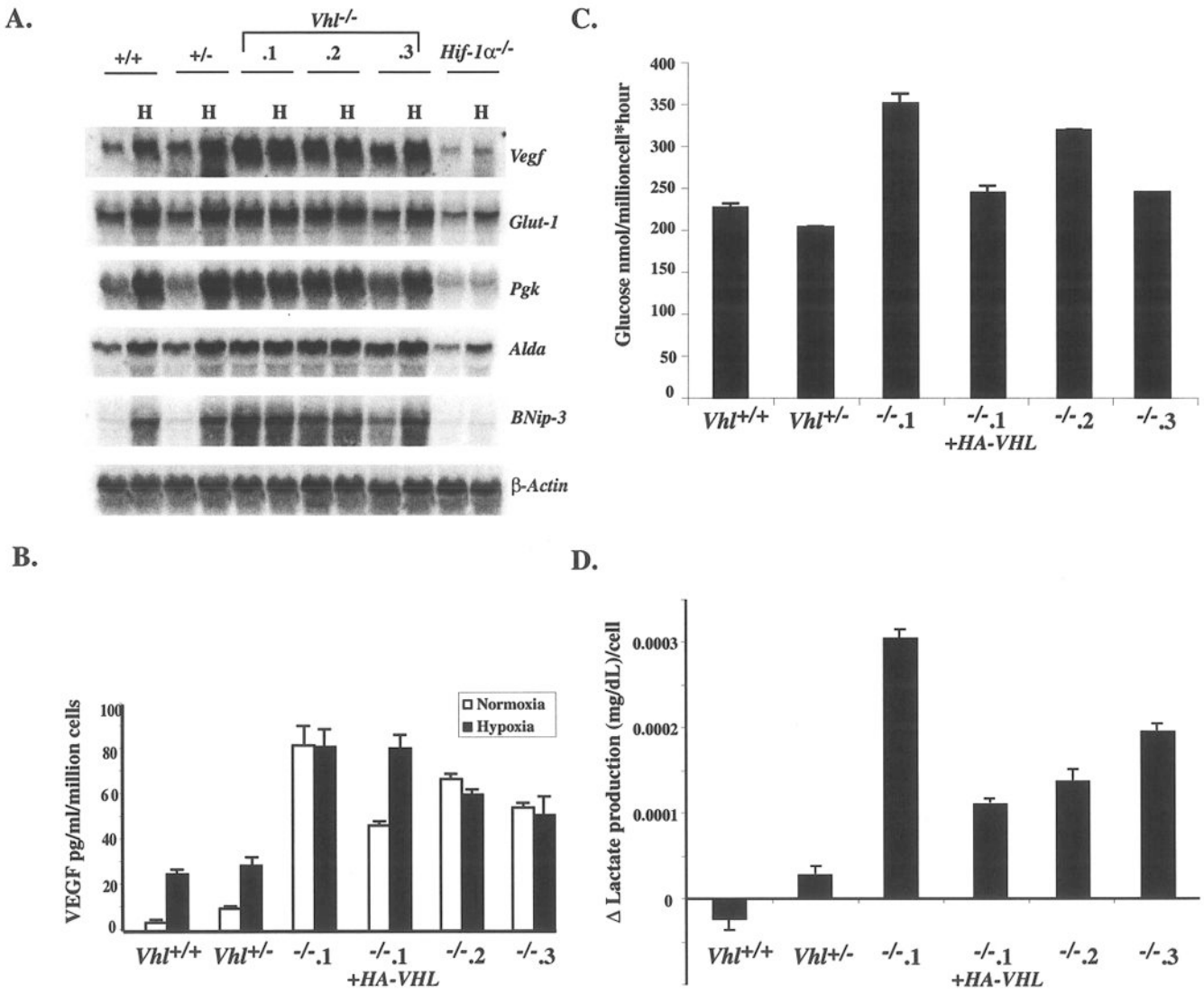


**Figure 4. Induction of HIF target genes in normoxic *Vhl*$^{-/-}$ ES cells**

A: Total RNA isolated from *Vhl* $^{+/+}$, *Vhl* $^{+/-}$, *Vhl*$^{-/-}$ clones and *Hif-1α*$^{-/-}$ ES cells was probed for *Vegf*, *Glut-1*, *Pgk*, *Alda*, *Bnip-3*, and *β-actin* , which served as a loading control. Expression of HIF target genes was abundant under normoxia and failed to be further induced by hypoxia in *Vhl*$^{-/-}$ ES clones. B: *In vitro* secretion of VEGF was measured by ELISA. VEGF secretion was greatly induced by hypoxia in *Vhl*$^{+/+}$ and *Vhl*$^{+/-}$ ES cells but not in *Vhl*$^{-/-}$ clones. The high level of VEGF secretion by *Vhl*$^{-/-.1}$ was suppressed by reintroduction of HA-VHL. C: A representative measurement of the glycolytic rate assessed as the rate of conversion of $^{3}$H-Glucose to $^{3}H_20$ (Liang *et al.* 1997). *Vhl*$^{-/-}$ ES cells consumed glucose at a higher rate than controls, which was suppressed by reintroduction of HA-VHL. D: Change in lactate secretion measured over the course of 24 hrs is depicted. *Vhl*$^{-/-}$ *ES* cells secreted greater amounts of lactate when compared to controls, which was rescued by reintroduction of HA-VHL. All assays were performed in triplicate and bars represent standard error.

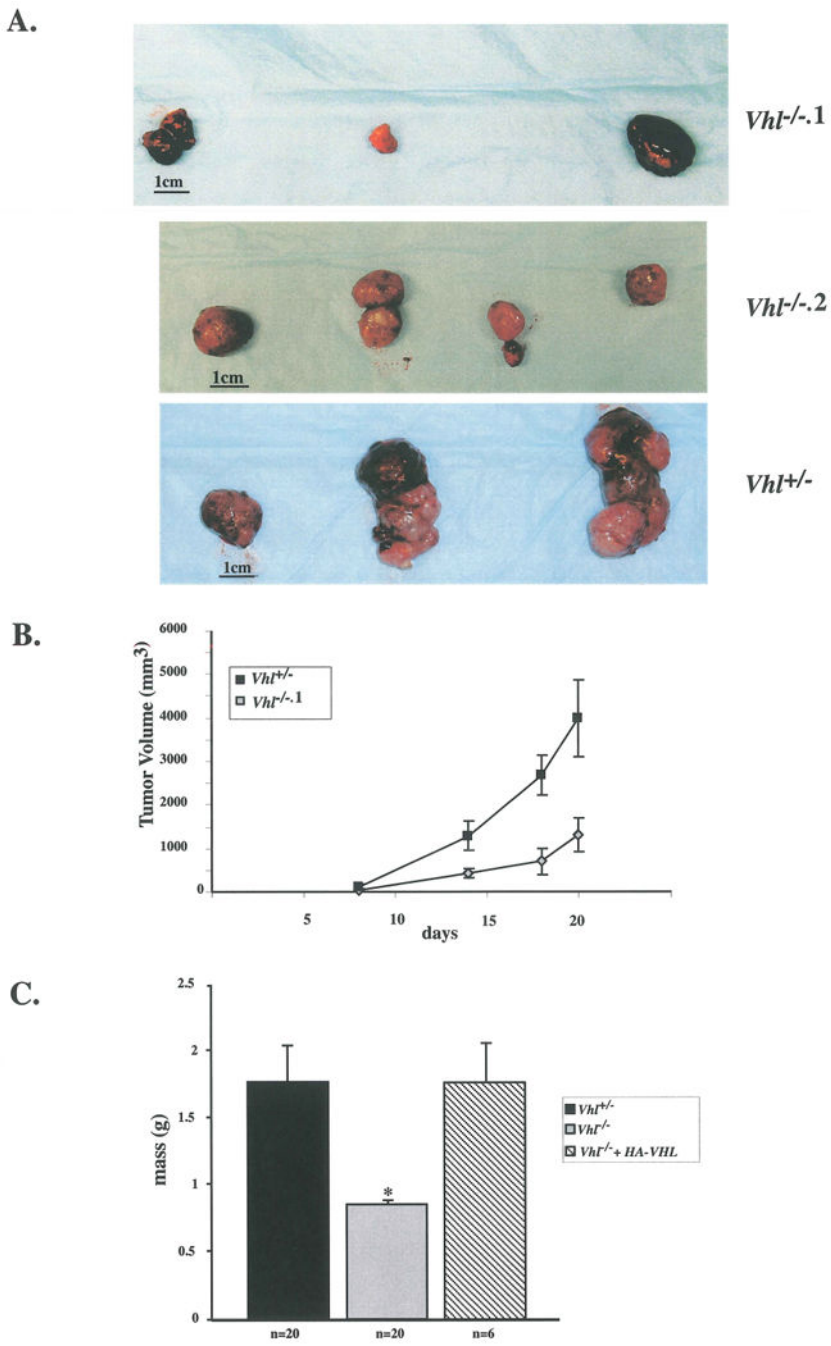


**Figure 5. Decrease in growth of *Vhl*$^{-/-}$ tumors**

A: Teratocarcinomas were created by injecting *VhV*$^{-/-}$, *Vhl*$^{-/-.1}$, and *Vhl*$^{-/-.2}$ ES cells subcutaneously into nude mice. *Vhl*$^{-/-}$ tumors ranged in size but were considerably smaller than *Vhl*$^{+/-}$ derived tumors. B: Rate of tumor growth was measured by tumor volume for 21 days. C: Graph represents the combined results of three separate experiments in which the masses of *Vhl*$^{+/+}$, *Vhl*$^{-/-}$, and *Vhl*$^{-/-.1}$ + HA-VHL tumors after 21 days of growth were measured. N values are as indicated and bars represent standard error. *Vhl*$^{-/-}$ tumors were significantly smaller than *Vhl*$^{+/-}$ derived tumors. Genetically rescued *Vhl*$^{-/-.1}$ + HA-VHL

tumors grew similarly to *Vhl*$^{+/-}$ tumors. Student t-test revealed a statistically significant difference between tumor masses, p=0.003.

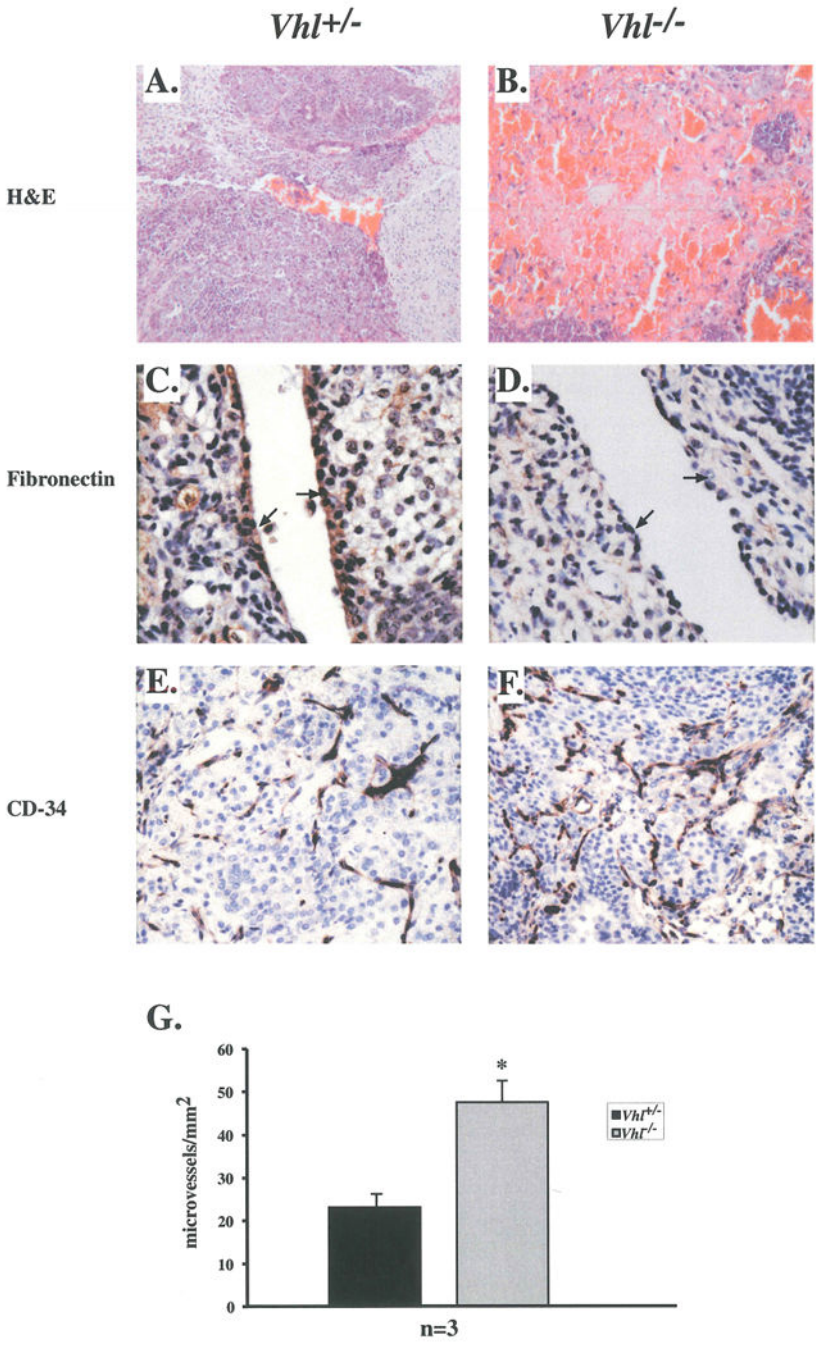


**Figure 6. Increased hemorrhagic regions and vasculature of *Vhl*$^{-/-}$ tumors**

A & B: Hematoxylin and eosin staining of *Vhl*$^{+/-}$ and *Vhl*$^{-/-}$ tumors. C & D: Basement membrane expression of fibronectin in *Vhl*$^{+/-}$ endothelial cells (arrows) and reduced fibronectin deposition in endothelial cells of *Vhl*$^{-/-}$ tumors (arrows). E: CD-34 staining of *Vhl*$^{+/-}$ microvessels. F: Microvessel density in *Vhl*$^{-/-}$ tumors appeared to be increased as demonstrated by α-CD-34 staining. G: Quantitation of tumor microvessel density. The microvessel density of *Vhl*$^{-/-}$ tumors was greater than controls, n=3. Student t-test revealed

statistically significant differences between tumor types, $p<0.03$. Bars represent standard error. Final magnifications are 100X (A and B), 400X (C and D) and 200X (E and F)

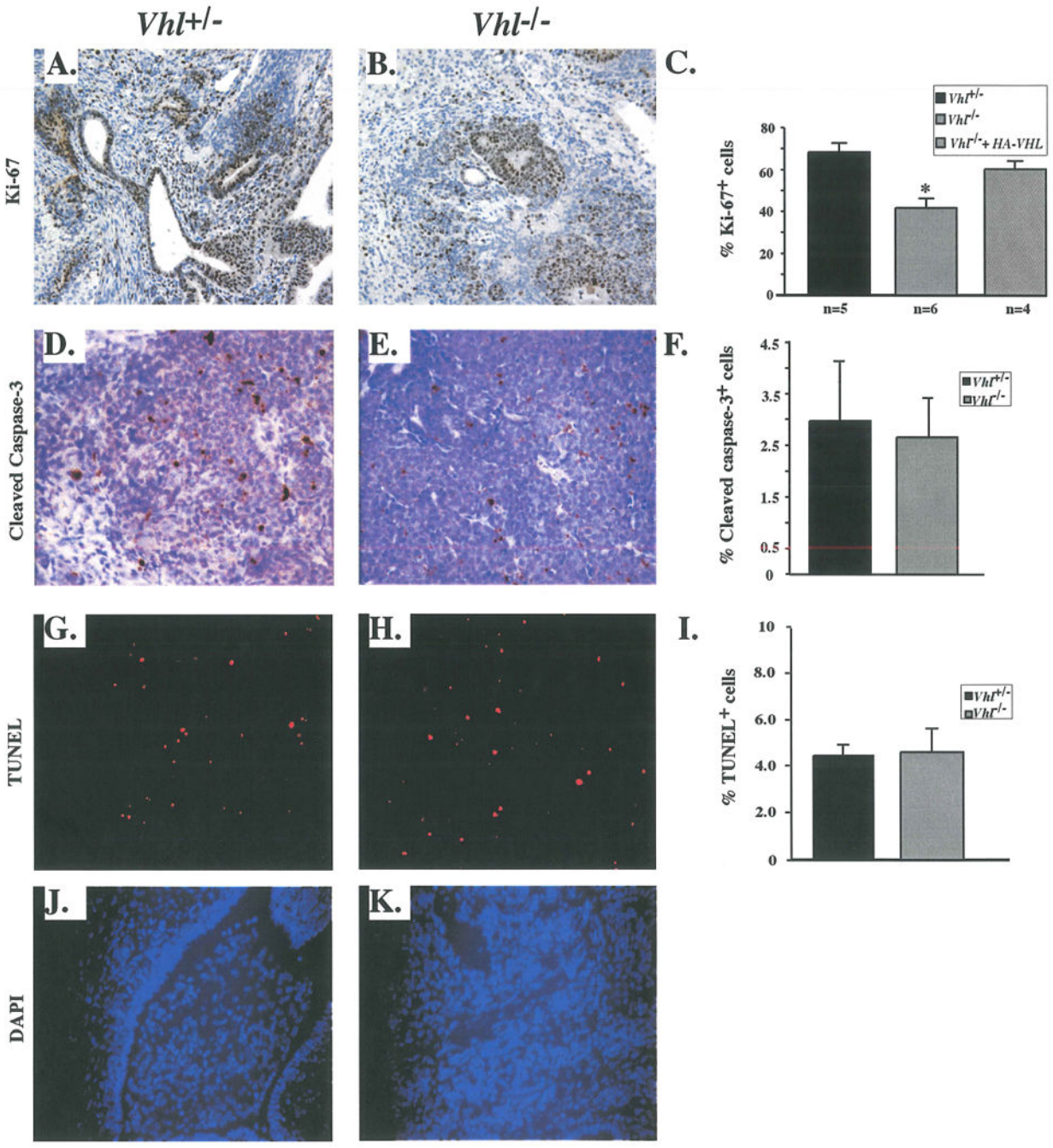


**Figure 7. *Vhl*$^{-/-}$ tumors exhibited a decrease in proliferation but no increase in apoptosis**

A: Proliferation marker Ki-67 indicated highly proliferating regions of *Vhl*$^{+/-}$ tumors. B: Expression of Ki-67 in *Vhl*$^{-/-}$ tumors was reduced compared to morphologically similar *Vhl*$^{+/-}$ regions. C: Quantitation of Ki-67$^{+}$ cells in *Vhl*$^{+/-}$, *Vhl*$^{-/-}$ and *Vhl*$^{-/-}$ + HA-VHL tumors. *Vhl*$^{-/-}$ tumors were less proliferative than controls. Student t-test revealed statistically significant differences between tumors types, $p < 0.003$. D& E: Expression of apoptotic marker cleaved caspase-3 in non-necrotic regions of *Vhl*$^{+/-}$ tumors. Cleaved caspase-3 staining was not increased in *Vhl*$^{-/-}$ tumors. F: Quantitation of cleaved caspase-3$^{+}$ cells in

*Vhl*$^{+/-}$ and *Vhl*$^{-/-}$ tumors. No significant differences were observed between genotypes. G & H: TUNEL staining demarcated apoptotic cells in non-necrotic regions of *Vhl*$^{+/-}$ and *Vhl*$^{-/-}$ tumors. I: Quantitation of TUNEL$^{+}$ cells in *Vhl*$^{+/-}$ and *Vhl*$^{-/-}$ tumors. No significant differences were apparent between genotypes. N values are as indicated and bars represent standard error. Magnifications 200X (A-H).

## Table 1

### $Vhl^{-/-}$ tumors are smaller than controls

| | Genotype | T/S[a] | Days | Mean Mass (g) |
|---|---|---|---|---|
| Exp. 1 | *Vhl*$^{+/-}$ | 6/6 | 21 | 3.052 ± 0.670 |
| | *Vhl*$^{-/-.1}$ | 5/6 | 21 | 1.036 ± 0.257 |
| Exp. 2 | *Vhl*$^{+/-}$ | 10/10 | 21 | 1.223 ± 0.238 |
| | *Vhl*$^{-/-.2}$ | 10/10 | 21 | 0.709 ± 0.092 |
| Exp. 3 | *Vhl*$^{+/-}$ | 5/5 | 21 | 1.62 ± 0.371 |
| | *Vhl*$^{-/-.1}$ | 4/4 | 21 | 0.53 ± 0.125 |
| | *Vhl*$^{-/-.1}$ + *HA-VHL* | 5/5 | 21 | 1.76 ± 0.296 |
| Exp. 4 | *Vhl*$^{+/-}$ | 5/5 | 28 | 4.96 ± 1.19 |
| | *Vhl*$^{-/-.1}$ | 3/4 | 28 | 0.466 ± 0.318 |

[a] T/S, number of tumors formed/ number of sites injected.